AD-A075 216   AEROSPACE CORP   EL SEGUNDO CA ELECTRONICS RESEARCH LAB   F/G 20/12
JOSEPHSON JUNCTION CHARACTERIZATION FROM IMPEDANCE MEASUREMENTS--ETC(U)
SEP 79   H KANTE   F04701-78-C-0079
UNCLASSIFIED   TR-0079(4727)-1   SAMSO-TR-79-54   NL

1 OF 1
ADA
075216

END
DATE
FILMED
11-79
DDC

LEVEL

Josephson Junction Characterization
from Impedance Measurements

Prepared by H. KANTER
Electronic Reseach Laboratory
Laboratory Operations
The Aerospace Corporation
El Segundo, Calif. 90245

DDC
OCT 19 1979
E

14 September 1979

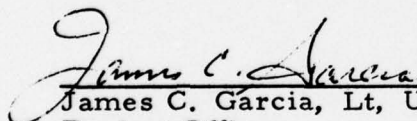Prepared for

OFFICE OF NAVAL RESEARCH
Washington, D.C. 22217

SPACE AND MISSILE SYSTEMS ORGANIZATION
AIR FORCE SYSTEMS COMMAND
Los Angeles Air Force Station
P.O. Box 92960, Worldway Postal Center
Los Angeles, Calif. 90009

AD A075216

DDC FILE COPY

79 10 17 007

This interim report was submitted by The Aerospace Corporation, El Segundo, CA 90245, under Contract No. F04701-78-C-0079 with the Space and Missile Systems Organization, Deputy for Technology, P.O. Box 92960, Worldway Postal Center, Los Angeles, CA 90009. It was reviewed and approved for The Aerospace Corporation by A. H. Silver, Director, Electronics Research Laboratory. Lieutenant J. C. Garcia, SAMSO/DYXT, was the project officer for Technology.

This report has been reviewed by the Information Office (OI) and is releasable to the National Technical Information Service (NTIS). At NTIS, it will be available to the general public, including foreign nations.

This technical report has been reviewed and is approved for publication. Publication of this report does not constitute Air Force approval of the report's findings or conclusions. It is published only for the exchange and stimulation of ideas.

James C. Garcia, Lt, USAF
Project Officer

George A. Kuck, Maj, USAF, Chief
Technology Plans Division

FOR THE COMMANDER

Burton H. Holaday, Col, USAF
Director of Technology Plans and
  Analysis
Deputy for Technology

SECURITY CLASSIFICATION OF THIS PAGE (When Data Entered)

REPORT DOCUMENTATION PAGE	READ INSTRUCTIONS BEFORE COMPLETING FORM

1. REPORT NUMBER	2. GOVT ACCESSION NO.	3. RECIPIENT'S CATALOG NUMBER
SAMSO-TR-79-54		

4. TITLE (and Subtitle)

JOSEPHSON JUNCTION CHARACTERIZATION FROM IMPEDANCE MEASUREMENTS

5. TYPE OF REPORT & PERIOD COVERED

Interim rept.

6. PERFORMING ORG. REPORT NUMBER

TR-0079(4727)-1

7. AUTHOR(s)

Helmut Kanter

8. CONTRACT OR GRANT NUMBER(s)

F04701-78-C-0079

9. PERFORMING ORGANIZATION NAME AND ADDRESS

The Aerospace Corporation
El Segundo, Calif. 90245

10. PROGRAM ELEMENT, PROJECT, TASK AREA & WORK UNIT NUMBERS

411279

11. CONTROLLING OFFICE NAME AND ADDRESS

Office of Naval Research
Washington, D.C. 22217

12. REPORT DATE

14 September 1979

13. NUMBER OF PAGES

24

14. MONITORING AGENCY NAME & ADDRESS(if different from Controlling Office)

Space and Missile Systems Organization
Air Force Systems Command
Los Angeles, Calif. 90009

15. SECURITY CLASS. (of this report)

Unclassified

15a. DECLASSIFICATION/DOWNGRADING SCHEDULE

16. DISTRIBUTION STATEMENT (of this Report)

Approved for public release; distribution unlimited

17. DISTRIBUTION STATEMENT (of the abstract entered in Block 20, if different from Report)

18. SUPPLEMENTARY NOTES

This report was formerly ATM-78(3727)-1.

19. KEY WORDS (Continue on reverse side if necessary and identify by block number)

20. ABSTRACT (Continue on reverse side if necessary and identify by block number)

Voltage biased junctions in SQUID type configurations show a characteristic response in their MW impedance, which as indicated by a small signal analysis appears primarily determined by the junction termination at the low frequency idler. The evaluation of the response affords the measurement of some circuit and junction parameters which cannot otherwise be obtained from I-V measurements and thus could be of considerable help in characterizing Josephson junctions in microwave circuits.

DD FORM 1473
(FACSIMILE)

SECURITY CLASSIFICATION OF THIS PAGE (When Data Entered)

392106

CONTENTS

Accession For

NTIS   GRA&I
DDC TAB
Unannounced
Justification

By

Distribution/

Availability Codes

Dist	Avail and/or special
A	

FIGURES

I. INTRODUCTION

If one measures the amplitude of the wave reflected from a junction placed in double hole SQUID fashion across a waveguide, with provisions to voltage bias the junction (Resistive SQUID), then the in phase and out of phase components vary with bias as shown in Fig. 1. The RSJ model qualitatively predicts an impedance variation of this type. However, in previous analyses[*,1] the out of phase component (or reactive portion) appeared only when the junction oscillations were locked to the probing signal. Reported impedance measurements[2] as well as our own observations on point contacts did not show any evidence of locking. As a matter of fact, in our experiments the self oscillations could occasionally be observed as hash on the center portion of the structure in Fig. 1. Thus locking definitely did not occur and another interpretation of the observed impedance variation with bias is required. A simple explanation may be provided by the RSJ model if terminations at i er frequencies, particularly that at the difference frequency between applied signal and self-oscillations, are taken into account. This interpretation has been explored by a small signal analysis, which is described in this communication. It reveals that, by measurement of the impedance of a biased junction, a number of junction and circuit parameters could be determined, which otherwise would not be accessible. It appears that these measurements, together with an I-V characteristic, would serve to completely characterize a junction and its immediate embedding network. The reason for this is the fact that with the junction self-oscillations we are able to provide a frequency sweep from essentially zero frequency to frequencies very large compared

---

[*]M. Kaminaga, "rf Impedance of Superconducting Weak Links," J. Phys. Soc. Japan, to be published.

[1]F. Auraches and T. Van Duzer, "rf Impedance of Superconducting Weak Links," JAP **44**, 848 (1973).

[2]D. E. Claridge, "rf Current Dependence of 8.9 GHz Impedance of Tantalum Point-Contact Josephson Junctions", JAP **48**, 1762 (1977).
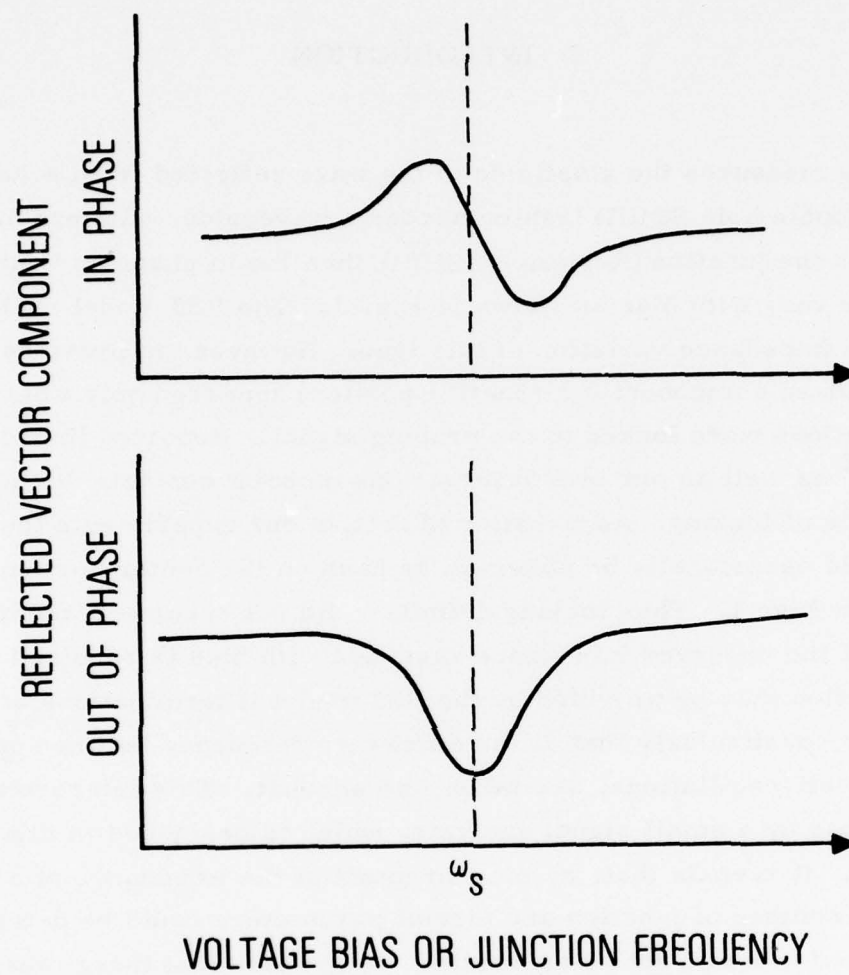
Fig. 1. Change is reflection when junction bias
is swept through probing frequency sig-
nal at ω_s

with the operating frequency; and, of course, frequency is an essential parameter in circuit evaluation. No other test system exists with the frequency versatility provided by a Josephson junction. Thus, it appears that the impedance evaluation could lead to quantitative determination of series inductance, junction capacitance, junction ohmic resistance at operating frequency, low frequency (DC) loop termination, and fundamental pump amplitude. An I-V characteristic would furthermore provide critical current and junction impedance at DC; and finally, the frequency profile of the self-oscillations at operating frequency would permit determination of the noise power in the circuit. This provides a rather complete junction description, lacking essentially only the spectrum of higher harmonics in the circuit. However, since the effects of subharmonic frequencies of the bias oscillations are observable in experiment, a more extended analysis might help to give some information on other harmonics in the circuits as well.

However, there exist various difficulties with the analysis presented here, and I have not been able to come to a satisfactory solution of these difficulties. They are pointed out in the respective sections of this note. As usual, refuge is sought in computer simulations, which should be better suited to treat the strong nonlinearities in the device. These studies are presently in progress on a computer with the aim to find out the validity of the results developed in the analysis. In case the numerical results bear out the analysis we should have some good junction-circuit diagnostics at hand; otherwise, the exercise might serve to at least give some indication of the qualitative functioning of the circuit.

II. ANALYSIS

We briefly derive the small signal approximation of the impedance for the RSJ model as it has previously been done by Vistavkin, et al.[3] and then include the effect of the terminations. We start with the circuit equation

$$\frac{V}{R_J} + I_c \sin \phi = I_o + I \sin \omega_s t \tag{1}$$

with the variables explained in Fig. 2. We assume $I \ll I_o$. I_o causes self-oscillations at ω_o with phase $\phi_o(t)$. The phase is modified by the small signal $\phi_1(t) \ll \phi_o(t)$. The linear 1st order approximation in reduced units is

$$\phi_1' + \cos \phi_o(t) \cdot \phi_1 = i \tag{2}$$

where $i = I/I_c$ and time is measured in units of $\omega_c^{-1} = \theta_o/I_o R_J$. Standard integration and the fact that $\cos \phi_o = -\phi_o''/\phi_o' = -\frac{d}{dt} \ln \phi_o'$ leads to the small signal voltage (in units $I_c R_J$)

$$v = i + \phi_o'' \int \frac{i}{\phi_o'} \, d\tau \tag{3}$$

The second term always gives a real (resistive) contribution which can become negative. Note that it describes a double mixing process with the self-oscillations by two 90° phase shifting processes: (a) integration and (b) multiplication with a 90° phase shifted voltage contribution (when only the fundamental

[3] A. N. Vistavkin, V. N. Gubankov, L. S. Kuzmin, K. K. Likharev, V. V. Migulin and B. K. Semenov, "S-c-S Junctions as Non-Linear Elements of Microwave Receiving Devices", Rev. Physique and Appliquee, 9, 79 (1974).
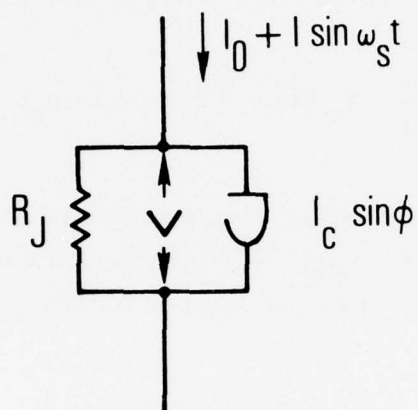
Fig. 2. Basic current driver
function circuit

frequency terms are considered). The fact that v, and thus the impedance v/i, is determined by the large voltage variation due to self oscillation and its derivative suggests that the above equation is of more general validity than applicable only for sin ϕ dependences. In fact it can be shown that it holds for any periodic I vs. ϕ dependence if an accommodation between super and normal current is enforced by the external circuit (See Appendix).

Using Eq. (3), one obtains an impedance matrix (in units of R_J) for the 3 main idler components (Fig. 3)

$$
\begin{bmatrix} v_s \\ v_{-1} \\ v_{-2} \end{bmatrix} = \begin{bmatrix} 1 - \dfrac{a - \overline{v}}{2\omega_{-1}} & \dfrac{a(a - \overline{v})}{\omega_{-1}} & -\dfrac{(a - \overline{v})}{2\omega_{-1}} \\ -\dfrac{1}{2\overline{v}} & +\dfrac{a}{\overline{v}} & -\dfrac{1}{2\overline{v}} \\ \dfrac{a - \overline{v}}{2\omega_{-1}} & \dfrac{a(a - \overline{v})}{\omega_{-1}} & 1 + \dfrac{a - \overline{v}}{2\omega_{-1}} \end{bmatrix} \begin{bmatrix} i_s \\ i_{-1} \\ i_{-2} \end{bmatrix} \tag{4}
$$

where it is assumed that small currents are injected at all three frequencies of interest and only terms have been retained which become large for $\omega_{-1} = \omega_s - \omega_o \to 0$, or 1st order terms if no singular term occurs. The matrix holds for the analytically tractable RSJ model with $I_s = I_c \sin \phi$, where the terms $(a - \overline{v})$, with $a = I_o/I_c$ and $\overline{v} = \sqrt{a^2 - 1}$, represent the Fourier component at ω_o, the pump frequency. In what follows, we replace $(a - \overline{v})$ with a more general amplitude coefficient $\gamma = \dfrac{a - \overline{v}}{2}$.

Using standard methods after inclusion of terminations (where the voltage-current relation is enforced by the external circuit) one obtains

$$
\begin{bmatrix} v_s \\ 0 \\ 0 \end{bmatrix} = \begin{bmatrix} 1 - \dfrac{\gamma}{\omega_{-1}} & \dfrac{2a\gamma}{\omega_{-1}} & -\dfrac{\gamma}{\omega_{-1}} \\ -\dfrac{1}{2\overline{v}} & \dfrac{a}{\overline{v}} + Z_{-1} & -\dfrac{1}{2\overline{v}} \\ \dfrac{\gamma}{\omega_{-1}} & \dfrac{2a\gamma}{\omega_{-1}} & 1 + \dfrac{\gamma}{\omega_{-1}} + Z_{-2} \end{bmatrix} \begin{bmatrix} i_s \\ i_{-1} \\ i_{-2} \end{bmatrix} \tag{5}
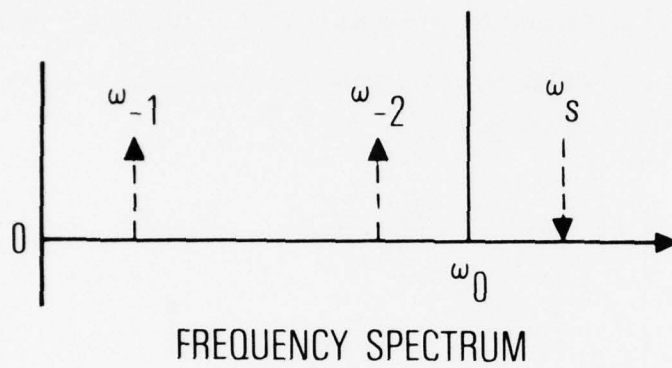$$

Fig. 3. Frequency components considered in
analysis. ω_S is applied frequency ω_{-1}
and ω_{-2} first and second idler fre-
quencies, respectively.

from which the impedance of the circuit at ω_s is obtained (with $\sigma = \frac{a}{\overline{v}} = \frac{R_D}{R_J}$ where R_D is the slope of I-V characteristic):

$$Z_s = \frac{1 - \dfrac{Z_{-1}}{\sigma + Z_{-1}} \dfrac{Z_{-2}}{1 + Z_{-2}} \dfrac{\gamma}{\omega_{-1}}}{1 + \dfrac{Z_{-1}}{\sigma + Z_{-1}} \dfrac{1}{1 + Z_{-2}} \dfrac{\gamma}{\omega_{-1}}} \tag{6}$$
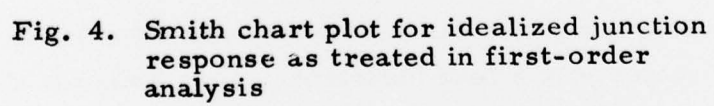
We now specify the termination at ω_{-1} as $Z_{-1} = j\omega_{-1}L_{DC}$ (in units R_J), where L_{DC} is the DC inductance of the circuit closing the junction current. Assuming for now $Z_{-2} = \infty$, we obtain

$$Z_s = 1 - \frac{j\omega_{-1}L_{DC}}{\sigma + j\omega_{-1}L_{DC}} \frac{\gamma}{\omega_c}$$

$$Z_s = R_J - \gamma L_{DC} \left\{ \frac{\omega_{-1}L_{DC}/R_J}{\left(\dfrac{\sigma}{R_J}\right)^2 + \omega_{-1}^2\left(\dfrac{L_{DC}}{R_J}\right)^2} + j \frac{\sigma/R_J}{\left(\dfrac{\sigma}{R_J}\right)^2 + \omega_{-1}^2\left(\dfrac{L_{DC}}{R_J}\right)^2} \right\} \tag{7}$$

This is the junction impedance in the vicinity of $\omega_o \approx \omega_s$. For $|\omega_{-1}| = |\omega_s - \omega_o| \gg R_D/L_{DC}$ the parenthesis vanishes and $Z_s \approx R_J$. At $\omega_{-1} = 0$ the reactive term is $-j \gamma L_{DC}/R_D$. The "half width" holds for $|\omega_{-1}^{(h)}| = R_D/L_{DC}$. From both these relations which can be determined experimentally, L_{DC}/R_D and γ can be determined.

The above quantities can readily be read off a Smith chart. We assume Z_s to be in series with a lead inductance, L_s. Thus, for $\omega_{-1} \gg R_D/L_{DC}$ and $\{\} \approx 0$ in Eq. 7, a point (L_s, R_J) is determined. When sweeping ω_o through ω_s, the $\{\}$ term assumes finite values and a circle is traced as shown in Fig. 4. Both circle diameter in terms of $\omega L_{DC}/Z_o$, and $\left(\omega_{-1}^{(1)} - \omega_{-1}^{(2)}\right)/2 = R_D/L_{DC}$ in terms of junction bias voltage, are obtained.

Fig. 4. Smith chart plot for idealized junction
response as treated in first-order
analysis

While the result presented is in qualitative agreement with experimental observations, the derivation contains a serious flaw. In case a real portion is considered in the impedance Z_{-1} of Eq. (6), no analytic expansion is obtained since a term ω_{-1} remains in the denominator, and, consequently, the term grows beyond bounds. Of course, in reality the junction generator at ω_{-1} has an internal impedance preventing singular behavior. One might suspect that as long as the external real load at ω_{-1} remains small compared with R_J, the analysis might give a reasonable description. Presently, numerical simulation is hoped to shed some light on this problem.

III. EXPERIMENTAL

In our 10 GHz, broad band, $Z_o \approx 5\Omega$ waveguide, we obtain a reflection response of just the type discussed above (see Fig. 5). Here we observe reflected vectors for constant input power at ω_s. Thus, consider the reflected vector normalized and the Smith Chart evaluation applies exactly. The observed inductance change is indeed negative. However, it is also apparent that the measured circle in response to bias variation is somewhat distorted. In what follows we indicate some reasons for this.

A.   We first consider the termination at ω_{-2}. Ignoring the series inductance, L_s, the junction near ω_s is essentially terminated by a short. Deviations to either higher or lower frequencies will result in capacitive or inductive loading of the junction at ω_{-2}. We have simulated the short with loading by a tank circuit, introducing at ω_s a load of form $Z_{-2} = jQ\frac{\Delta}{\omega_s}$ where $\Delta = \omega_{-2} - \omega_s \equiv 2\omega_{-1}$. This idler loading is evaluated with Eq. (6) and results in a circle distortion as shown in Fig. 6. We see distortion towards larger vectors for $\omega_o \gtrless \omega_s$ with no effect at $\omega_o = \omega_s$ in qualitative agreement with experimental indication (Fig. 5).

B.   The clearly observable distortions near the origin of the circle (curl-in at $Z \approx L_s$, R_J) are not described by the model. Since our approximation holds only for $\omega_o \approx \omega_s$, this is not particularly surprising.

C.   Since we are dealing here with a "variable" inductance at ω_s it should enable one to determine the capacitance of the junction. If the assumption is made that, in a circuit as sketched in Fig. 7a, the capacitance does not affect the general junction response with bias as determined by the termination at ω_{-1}, but enters only into the external circuit, then it can be shown by simple circuit analysis that the response circle is tilted on the Smith chart as shown in Fig. 8. Considering only the circle origin* and the point for $\omega_o = \omega_s$, we

---

*Circle origin is that point obtained for the ideal model where $\omega_o \to o$ or $\omega_o \gg \omega_s$.
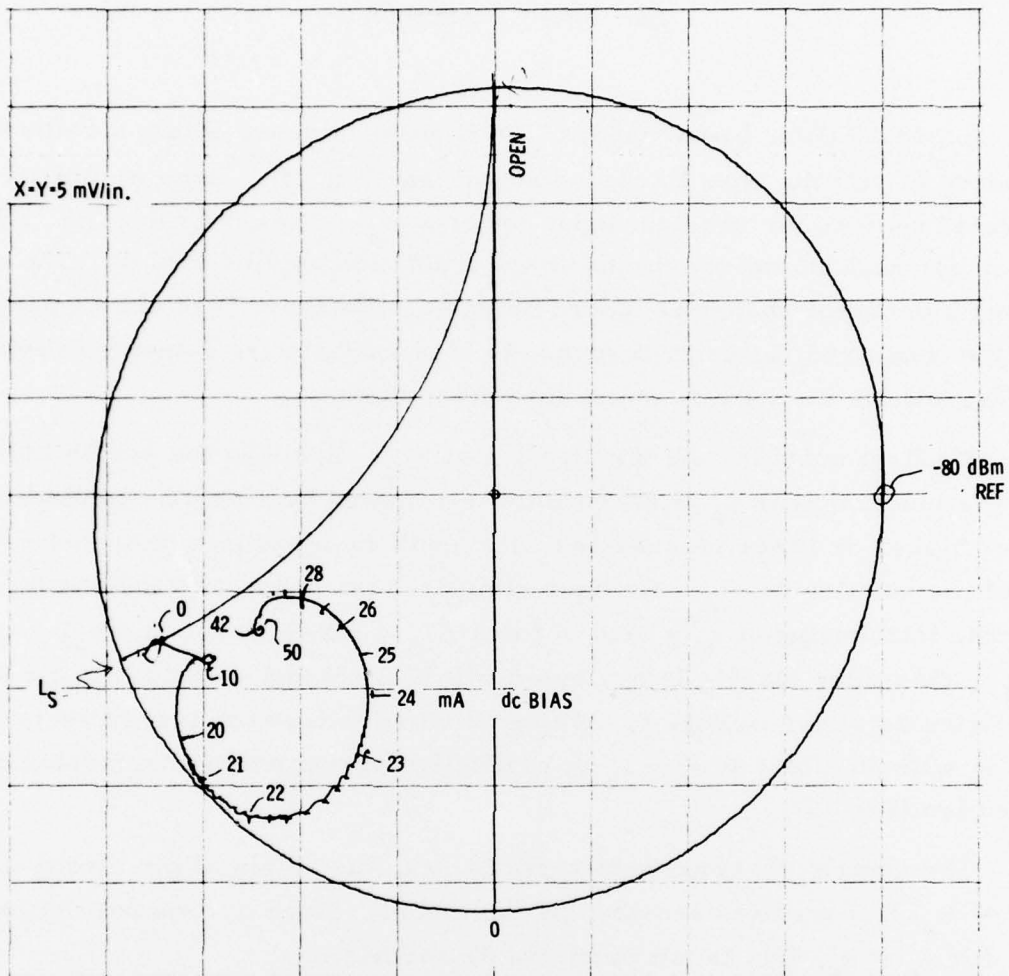
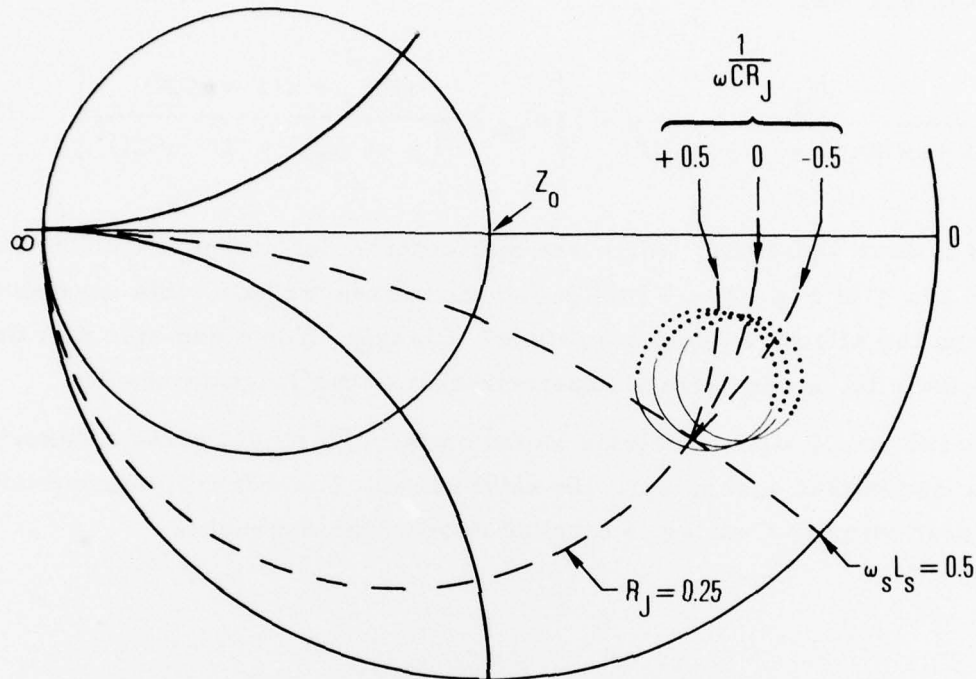Fig. 5. Measured junction response in Smith
chart presentation

Fig. 6. Modification of idealized response (Fig. 4) due to second idler termination where $\lambda/4$ short termination is approximated with lumped resonance circuit with resonance at ω_s.

can now read off four values (two for the origin, two for $\omega_o = \omega_s$). These values determine real and imaginary parts of the expressions derived from the circuit of Fig. 7a:

$$Z = \frac{R_J}{\left(1 + \omega CR_J\right)^2 + (1 + \omega CX)^2} + j\left\{\omega L_S - \frac{\omega CR_J^2 + X(1 + \omega CX)}{\left(1 + \omega CR_J\right)^2 + (1 + \omega CX)^2}\right\} \quad (8)$$

The result is four equations, which are sufficient to determine the unknowns L_S, R_J, C and X of Fig. 7a. From X and the measured half width we deduce R_D/L_{DC} and the effective pump amplitude. Clearly, if one can also plot the I-V characteristic, a complete characterization of the junction results.

Thus the small signal analysis based on the RSJ model gives a description in fair qualitative agreement with experiment. The difficulty encountered with the assumption in C above is touched upon in the appendix.
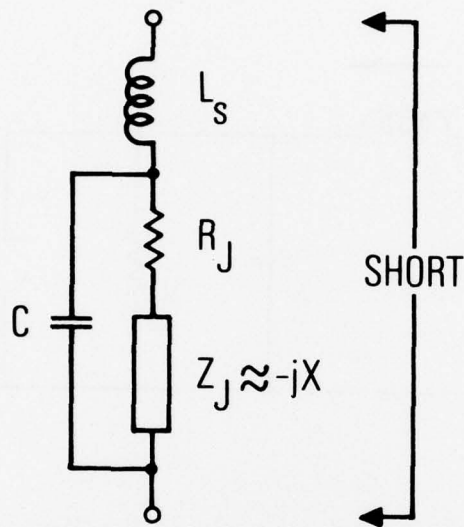
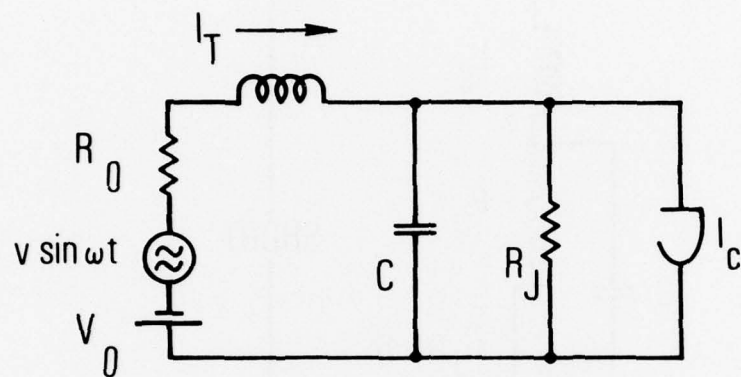Fig. 7a. Junction embedding network where junction varies as Z_y.

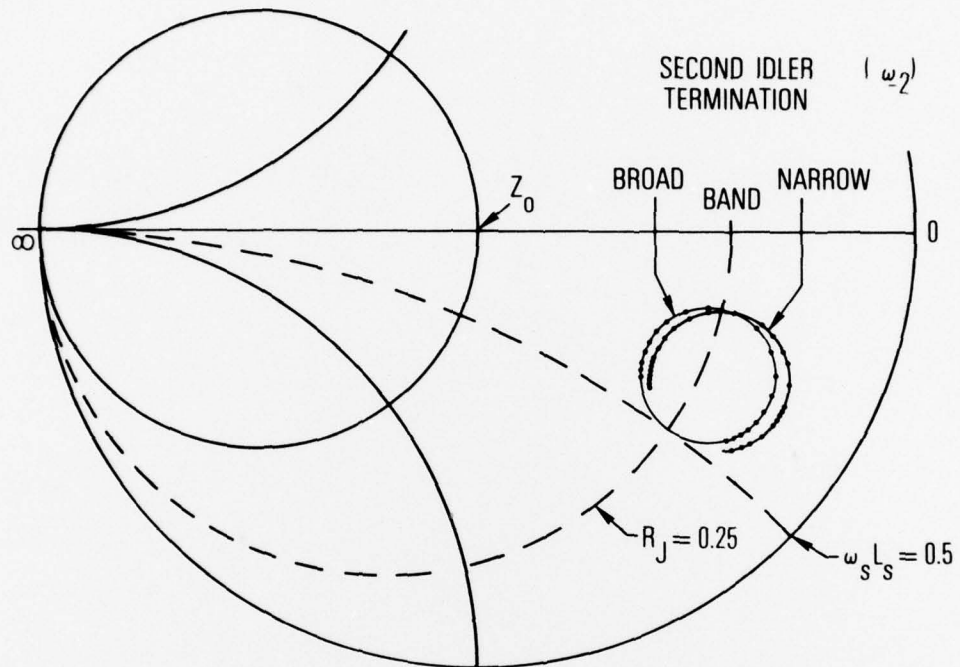Fig. 7b. Junction embedding network where junction is represented by I_c and R_j.

Fig. 8. Modification of idealized response (Fig. 4) by
capacitive loading.

APPENDIX

Here we show to what extent a periodic supercurrent-phase relation always results in a real contribution to biased junction impedance. Suppose the junction (with no capacitance) is driven by a DC current in RSJ model fashion; the differential equation for the phase evolution then is

$$\phi'_o + f(\phi_o) = \text{const} \tag{1B}$$

when written in reduced units and when the usual $\sin \phi_o$ term is replaced by an arbitrary periodic function, $f(\phi_o)$. The response to a <u>small</u> ac current injected in addition to the DC current results in

$$\phi'_o + \phi'_1 + f(\phi_o + \phi_1) = \text{const} + \Delta i \tag{2B}$$

or, after expansion to first order and use of Eq. (1B),

$$\phi'_1 + \frac{df}{d\phi} \Big|_o \phi_1 = \Delta i \tag{3B}$$

On the other hand $df/d\phi|_o$ may also be obtained from Eq. (1B) by differentiation with respect to time:

$$\phi''_o + \frac{df}{d\phi} \phi'_o = 0 \tag{4B}$$

from which

$$\frac{df}{d\phi} = -\frac{\phi''_o}{\phi'_o} = -\frac{d}{dt} \ln \phi'_o \tag{5B}$$

and consequently Eq. (3B) may be written

$$\phi'_1 - \left(\frac{d}{dt} \ln \phi'_o\right)\phi_1 = \Delta i \tag{6B}$$

Standard methods for solving a first order linear differential equation
$\phi'_1 + g(t)\phi_1 = \Delta i$ result in

$$\phi_1(t) = - \exp^{-\int g\, dt} \cdot \int \exp^{\int g\, dt} \Delta_i\, dt + Q \exp^{-\int g\, dt}$$

or, with Eq. (6B)

$$\phi_1(t) = \phi'_o \int \frac{\Delta i}{\phi'_o}\, dt + Q\, \phi'_o$$

and

$$v = \phi'_1(t) = \phi''_o \int \frac{\Delta i}{\phi'_o}\, dt + \Delta i \tag{7B}$$

where we choose initial conditions such that $Q = 0$. Assuming only the funda-
mental Fourier components of ϕ'_o and ϕ''_o to be of significance, it is easily
verified that the first term of Eq. (7B) generates in phase components only.
We now briefly consider the more general case where the junction is em-
bedded in the circuit of Fig. 7b. The starting equations are

$$CV + \frac{V}{R_J} + I_c S(\phi) = I_T \tag{8B}$$

$$L \frac{d}{dt} I_T + I_T R_o + V_o + V = 0 \tag{9B}$$

-26-

After integration of Eq. (9B) and insertion into Eq. (8B) we find

$$CV + \frac{V}{R_J} + I_c S(\phi) + \frac{1}{L} \exp{-\frac{R_o}{L} t} \int V \exp{\frac{R_o}{L} t} \, dt = \frac{V_o}{R_o} \qquad (10B)$$

We approximate the 4th term by setting in it $V = \bar{v} + v \cos \omega_o t$ and obtain

$$\frac{\bar{v}}{R_o} + \frac{\bar{v}}{\omega_o} \frac{1}{\left(\frac{R_o}{\omega_o L}\right)^2 + 1} \left(\frac{R_o}{\omega_o L} \sin \omega_o t - \cos \omega_o t\right) \qquad (11B)$$

With $\omega_o L \ll R_o$ we may neglect the $\cos \omega_o t$ contribution. Then the second portion of Eq. (11B) becomes

$$\frac{\omega_o L}{R_o} \int v \cos \omega_o t \, dt$$

Eq. (10B) can then be written in reduced units

$$\beta_c \phi'' + \phi' + S(\phi) + \frac{\omega_o L}{R_o} \frac{1}{\beta} \phi = \frac{V_o - \bar{v}}{R_o I_c} \, . \qquad (12B)$$

where

$$\beta_c = hC/I_c 2e$$

$$\beta = h/2eI_c L$$

Note that

$$\frac{\omega_o L}{R_o} \frac{1}{\beta} = \frac{\omega_o}{\omega_c} \frac{R_J}{R_o} \qquad (13A)$$

which for a properly loaded junction with $\omega_o L_J \approx R_o$ is of order one; therefore even for small $\omega_o L \ll R_o$ the term is usually not negligible. Furthermore $\bar{v}$ in the right hand side changes to second order only with application of a small disturbance in $V_o \rightarrow V_o + \Delta v_s \cos \omega t$. If we set $\beta_c = 0$, the linearized small signal approximation of Eq. (12B) is of the same form as Eq. (1B) and we may again write the solution

$$v = \phi_1'(t) = \phi_o'' \int \frac{1}{\phi_o'} \frac{\Delta v_s}{I_c R_o} \cos \omega_s t \, dt + \frac{\Delta v_s}{I_c R_o} \cos \omega_s t \qquad (13B)$$

Clearly the same conclusions apply as before for the current driven junction. The junction impedance is essentially real and modification due to idler loading as described in the main test should apply. The L in series with the junction does not modify the basic result.

Here, the difficulty arises in asserting that the analysis applies also when $C \neq O$ or $\beta_c \neq O$. When only supercurrent and an ohmic path is provided by the junction, with the requirement that the sum total remains constant, the above analysis applies. Clearly, the reasoning cannot hold any longer if an additional, reactive bypass is provided. Again, since the mathematics become complicated, it might be more economical to test with numerical simulation. The results of this simulation will be reported at a later time.

LABORATORY OPERATIONS

The Laboratory Operations of The Aerospace Corporation is conducting experimental and theoretical investigations necessary for the evaluation and application of scientific advances to new military concepts and systems. Versatility and flexibility have been developed to a high degree by the laboratory personnel in dealing with the many problems encountered in the nation's rapidly developing space and missile systems. Expertise in the latest scientific developments is vital to the accomplishment of tasks related to these problems. The laboratories that contribute to this research are:

Aerophysics Laboratory: Launch and reentry aerodynamics, heat transfer, reentry physics, chemical kinetics, structural mechanics, flight dynamics, atmospheric pollution, and high-power gas lasers.

Chemistry and Physics Laboratory: Atmospheric reactions and atmospheric optics, chemical reactions in polluted atmospheres, chemical reactions of excited species in rocket plumes, chemical thermodynamics, plasma and laser-induced reactions, laser chemistry, propulsion chemistry, space vacuum and radiation effects on materials, lubrication and surface phenomena, photosensitive materials and sensors, high precision laser ranging, and the application of physics and chemistry to problems of law enforcement and biomedicine.

Electronics Research Laboratory: Electromagnetic theory, devices, and propagation phenomena, including plasma electromagnetics; quantum electronics, lasers, and electro-optics; communication sciences, applied electronics, semiconducting, superconducting, and crystal device physics, optical and acoustical imaging; atmospheric pollution; millimeter wave and far-infrared technology.

Materials Sciences Laboratory: Development of new materials; metal matrix composites and new forms of carbon; test and evaluation of graphite and ceramics in reentry; spacecraft materials and electronic components in nuclear weapons environment; application of fracture mechanics to stress corrosion and fatigue-induced fractures in structural metals.

Space Sciences Laboratory: Atmospheric and ionospheric physics, radiation from the atmosphere, density and composition of the atmosphere, aurorae and airglow; magnetospheric physics, cosmic rays, generation and propagation of plasma waves in the magnetosphere; solar physics, studies of solar magnetic fields; space astronomy, x-ray astronomy; the effects of nuclear explosions, magnetic storms, and solar activity on the earth's atmosphere, ionosphere, and magnetosphere; the effects of optical, electromagnetic, and particulate radiations in space on space systems.

THE AEROSPACE CORPORATION
El Segundo, California

. . .